

## An obstacle avoidance path planner for an autonomous tractor using the minimum snap algorithm

Xin Zhao<sup>a,b</sup>, Ke Wang<sup>a,b</sup>, Sixian Wu<sup>a,b</sup>, Long Wen<sup>a,b</sup>, Zhibo Chen<sup>a,b</sup>, Liang Dong<sup>a,b</sup>, Mengyao Sun<sup>c</sup>, Caicong Wu<sup>a,b,\*</sup>

<sup>a</sup> College of Information and Electrical Engineering, China Agricultural University, Beijing 100083, China

<sup>b</sup> Key Laboratory of Agricultural Machinery Monitoring and Big Data Application, Ministry of Agriculture and Rural Affairs, Beijing 100083, China

<sup>c</sup> Beijing Agricultural Machinery Experiment Appraisal Extension Station, Beijing 100079, China



### ARTICLE INFO

**Keywords:**

Minimum snap algorithm  
Autonomous tractor  
Obstacle avoidance path planning  
Optimization model

### ABSTRACT

Autonomous tractors use a GNSS-based approach combined with other sensors to provide higher efficiency and minimize human intervention. The basis of field automated navigation is the agricultural route planning of the entire field. One of the main aspects of agricultural route planning is obstacle avoidance path planning, which can provide a safe continuous trajectory for autonomous tractors to pass obstacles. In this study, a collision-free path planning method was proposed using the minimum snap algorithm to enable the tractor to safely navigate from one point to another. To authenticate the proposed algorithm, a tripartite experimental scheme was designed, encompassing a ROS-based simulation, robot platform validation, and a field test. Simulation results demonstrate that the collision-free path generated by the proposed algorithms can effectively guide the tractor to follow the given path with a lateral error of 1.75 cm. For the robot platform validation test, the mean lateral deviations were 2.63 cm, 5.01 cm, and 6.80 cm at speeds of 0.5 m/s, 0.8 m/s, and 1.0 m/s, respectively. The feasibility of using the developed algorithms was followed by a field test with a 162-KW CVT autonomous tractor. The mean lateral deviations were 5.17 cm, 5.13 cm, and 6.10 cm at speeds of 0.6 m/s, 0.8 m/s, and 1.0 m/s, respectively. The test results showed that the model could provide a safe and stable collision-free path for agricultural machines operating in the field.

### 1. Introduction

In recent years, autonomous machines have been applied to agricultural tasks to improve work efficiency, relieve labor intensity, reduce labor costs, and enhance the quality of agricultural production (Ma et al., 2022). Path planning is one of the main tasks in the management of agricultural machinery, which can optimize the operation time, guarantee safety, and minimize the distance of traversing the entire area (Wang et al., 2022). Various applications use agricultural routing planning, such as crop harvesting (He et al., 2018), orchard navigation (Bochtis et al., 2015), and seeding tasks (Xiong et al., 2017).

In the context of smart farming, research in autonomous navigation has focused mainly on coverage path planning (CPP) approaches (Moysiadis et al., 2020). CPP methods are applied to generate routes traversing all field waypoints, especially in irregularly shaped terrains (Bochtis and Sørensen, 2009). Many researchers have provided various

approaches to minimize the distance of a route that passes the field tracks through work width, the turning radius of a machine, and other parameters (Bochtis and Vougioukas, 2008; Oksanen and Visala, 2009; Utamima et al., 2018). Bochtis et al. (2015) developed a route planning approach for intra- and inter-row orchard operations based on an optimal area coverage method for arable farming operations. Zhou et al. (2014) developed agricultural operations planning in the field with multiple obstacle areas, which requires low computation time to compute the optimal block sequence.

However, it is not always possible to satisfy all these requirements in complex environments. Furthermore, not all agricultural applications involve field-track following and headland-turning in free space. For instance, autonomous agricultural vehicles may have to move from one field to another, avoiding known collisions such as fences, trees, and barns, or they may operate inside nonempty structures such as greenhouses. Collision-free navigation is a fundamental requirement for the

\* Corresponding author.

E-mail addresses: zhao@cau.edu.cn (X. Zhao), wangke970406@163.com (K. Wang), sixianwu@cau.edu.cn (S. Wu), wl@cau.edu.cn (L. Wen), chenzb@cau.edu.cn (Z. Chen), dongliang@cau.edu.cn (L. Dong), 1228530516@qq.com (M. Sun), wucc@cau.edu.cn (C. Wu).

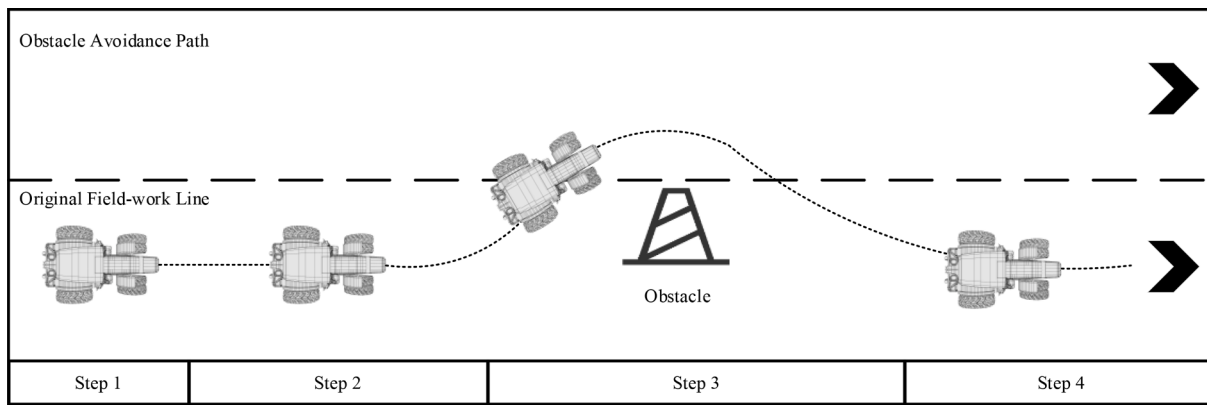


**Fig. 1.** The process of obstacle avoidance.

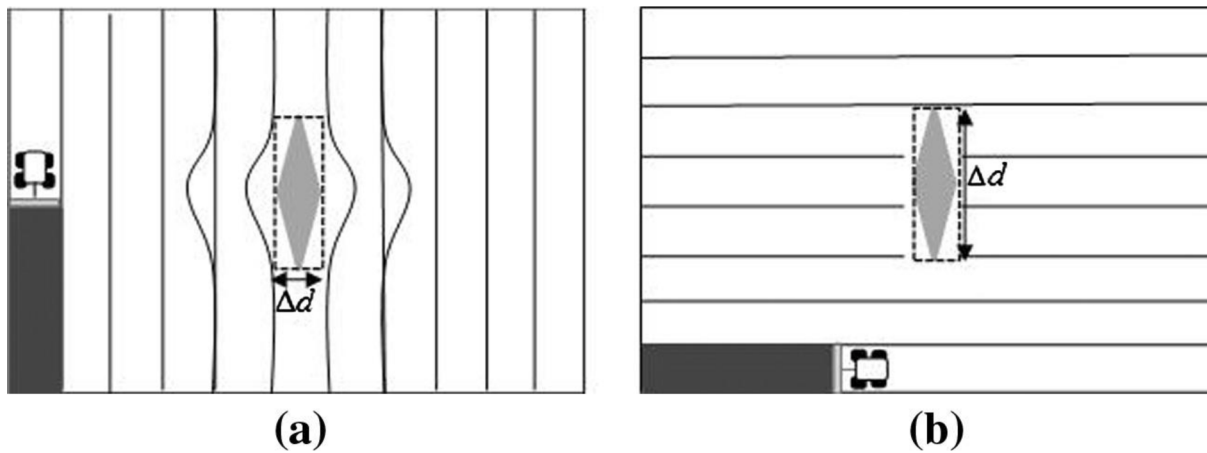


**Fig. 2.** The same collision can be considered different types depending on the driving direction (Zhou et al., 2014). Building upon the global path planning depicted in Figure (a), obstacle avoidance path planning exhibits better performance than the one shown in Figure (b).

unmanned operation of agricultural machinery, ensuring safety in complex farmland environments.

Obstacle avoidance path planning methods can be divided into four categories: graph search-based algorithms, sampling-based methods, interpolating curve planners, and numerical optimization approaches. The Dijkstra algorithm is a typical graph search algorithm that finds a single-source shortest path between two points. It had an outstanding performance in the DARPA challenge (Bohren et al., 2008). The A\* algorithm is an extension of the Dijkstra algorithm, which enables a fast node search due to the implementation of heuristics (Chabini and Lan, 2002). It has been applied in a wide range of applications (Abdallaoui et al., 2022), and its highlights are the node weights and the defined cost function. Although the two algorithms are practical, the path is discontinuous, and agricultural robot kinematics are not considered. To overcome these drawbacks, prior literature has provided many improved solutions. Jeon et al. (2021) proposed an entry-exit path planning method for an unmanned tractor operating in a paddy field using the A\* algorithm. They generated virtual obstacles to induce the A\* algorithm to determine the required operation curved path. Santos et al. (2019b, 2019a) introduced an extension to the A\* algorithm for ensuring a safe path in steep slope vineyards. The Probabilistic Roadmap Method (PRM) and Rapidly Exploring Random Tree (RRT) are the most common sampling-based approaches in robotics (Kavraki et al., 1996; LaValle and Kuffner, 2001). RRT has the capability of fast planning with nonholonomic constraints in semi-structured spaces by executing a random search (González et al., 2016). Vougioukas et al. (2006) utilized the RRT algorithm to explore the space of possible motions and compute a feasible trajectory, which offers a practical tool for planning point-to-

point motions for agricultural vehicles. However, the sampling-based solution is suboptimal and not curvature continuous, which does not match the demands of the autonomous tractor. Interpolating curves, such as Bezier curves, polynomial curves, Dubins curves, and other spline curves, are smooth and continuous paths. They are valuable approaches for generating the path by considering the initial and final states, which have low computational costs. Hameed. (2018) proposed a complete coverage path planning method using the Dubins curve to connect field tracks over the headland region. Thamrin et al. (2022) developed the Bezier-based curve to maneuver the unmanned vehicle on the planned path and maintain its position in the middle to avoid collision with existing trees or landmarks. Santos et al. (2022) developed a collision avoidance considering an iterative Bézier based approach for vineyard scenarios. However, for interpolating curves, more control points or higher degrees are required to make the planned path smoother and more continuous, increasing the computational burden (Zhang et al., 2021). Numerical optimization approaches minimize or maximize a function subject to various constrained variables. They include the artificial potential field method, discrete optimization, and the optimal control algorithm (Zhang et al., 2021). Ziegler et al. (2014) aimed to find a local, continuous process by minimizing an objective function that considers position, velocity, acceleration, and jerk as parameters. However, most of these methods only apply to on-road scenarios (Godoy et al., 2022). Yang et al. (2022a) used reinforcement learning algorithms in agricultural scenarios. A framework that tackles issues of environment mapping and path generation hierarchically was proposed (Lei et al., 2022). But they could not find one path planner that was considered safe, comfort, and collision-free on agricultural robotics.

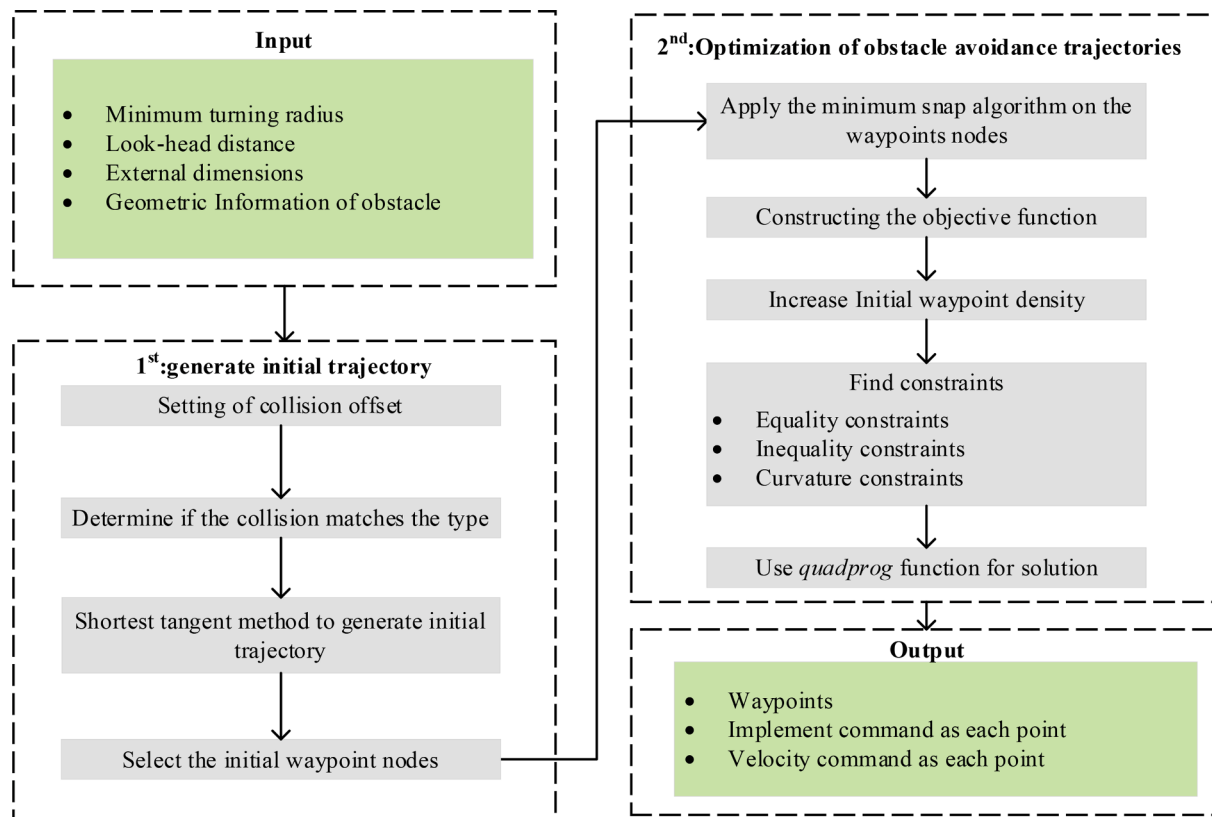


**Fig. 3.** Flowchart of the obstacle avoidance path planning method.

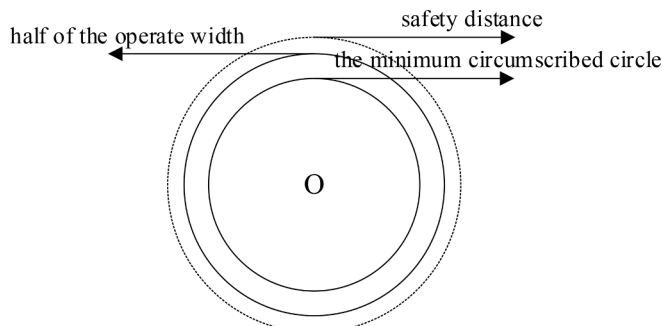


**Fig. 4.** Obstacle Feature Circle (OFC), refers to a geometric element that can be used to describe the position of an obstacle and define its safe distance.

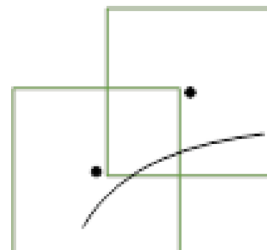


**Fig. 6.** The optimization area.

The objective of this paper was to develop a planning method that generates a feasible and collision-free path plan for agricultural machines using the minimum snap algorithm. The kinematic, position and curvature constraints are considered in the given objective function. We test the proposed method, mobile platform validation, and field

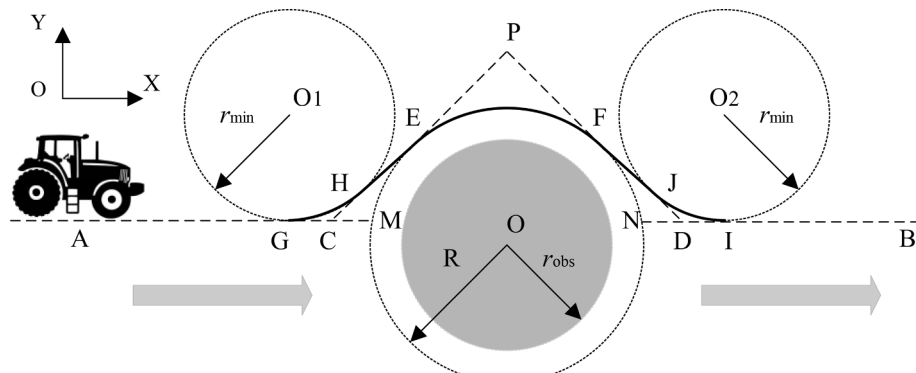


**Fig. 5.** The initial path based on the OFC.

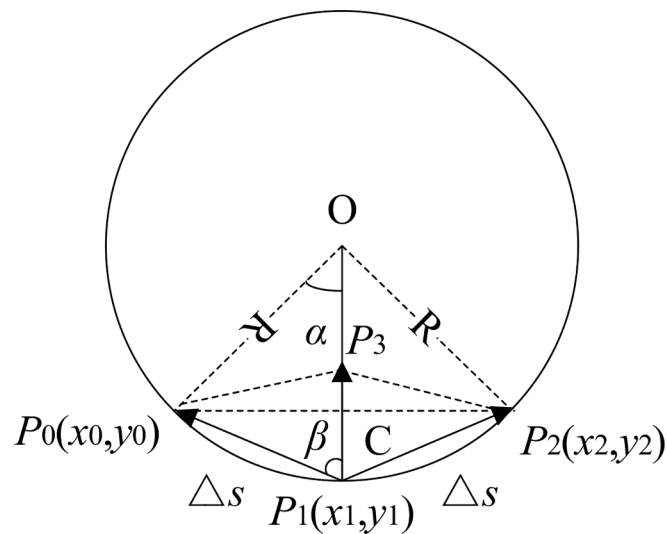


Fig. 7. Curvature circle.

experiment in the virtual environment.

## 2. Materials and methods

To analyze the process of obstacle avoidance, Section 2.1.1 analyzes the agricultural machine obstacle avoidance strategy and describes the technical process. Sections 2.1.2-2.1.3 introduce the path planner approach. To verify the usability of the algorithm, ROS simulation, mobile robot test, and field experiments are presented in Sections 2.2, 2.3, and 2.4, respectively.

### 2.1. Development of the obstacle avoidance path planner

Collision-free path planning can be described by a set of waypoints representing the path from the start point to the endpoint. Obstacle avoidance behavior consists of four sub-behaviors, as shown in Fig. 1.

Step 1: Obstacle avoidance detection: Determine if the tractor's current situation matches the criteria of the obstacle. If the tractor is operating in the field, the obstacle type is divided into four categories from type A to type D, which refers to Zhou et al. (2014). The same obstacle can be classified into different types depending on the driving

direction, as shown in Fig. 2. Otherwise, the tractor can prepare for obstacle avoidance.

Step 2: Path planning and look-ahead distance determination: A safe, smooth, and comfortable path is generated according to environmental information. A large look-ahead distance can lead to early steering and result in a large lateral error. In contrast, small look-ahead distances can cause the tracking process to oscillate back and forth near the reference path, resulting in an unstable tracking state (Yang et al., 2022b).

Step 3: Passing obstacle: The agricultural machinery passes around the obstacle based on the trajectory.

Step 4: Return to the original fieldwork path: The tractor returns to the original fieldwork track and continues to operate the remaining task.

#### 2.1.1. Overview of the obstacle-avoidance path planner

The obstacle avoidance approach consists of two stages, as shown in Fig. 3. In the first stage, the offset for the obstacle is determined by the geometric information of the obstacle and the main parameters of the agricultural machinery. After judging whether the block fits the category mentioned above, the shortest target method generates the initial trajectory, which provides the control points for the next stage. Although the shortest target method is simple to develop, the path is a line that does not satisfy the non-integrity constraint of the agricultural machinery and cannot be adequately tracked. In the second stage, the minimum snap algorithm was applied to the initial waypoints, from the start to the end. The object function was constructed using position, velocity, jerk, and snap, where safety and kinematic constraints were considered. The multicriteria optimization problem can be defined as a convex quadratic program, which a QP solver can address.

#### 2.1.2. The method of suboptimal path

The numerical optimization approach requires an initial feasible solution before obtaining the optimal trajectory. The obstacle avoidance region can be described by the Obstacle Feature Circle (OFC), as shown in Fig. 4. The OFC includes three layers. The inner layer is the minimum circumscribed circle of the obstacle. Simplification of collision can reduce the calculation burden. Its central position and radius can be obtained from the 3D field model, which can be generated by aerial photogrammetry. The middle layer depends on the operating width and is set to half of the width. The final expansion safety distance acts as the outer layer, providing an optimizable safety space as a buffer region.

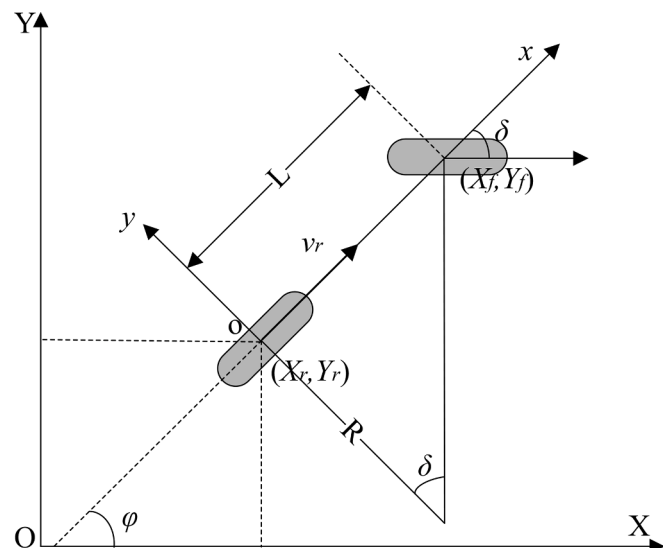


Fig. 8. Geometry of a bicycle model.

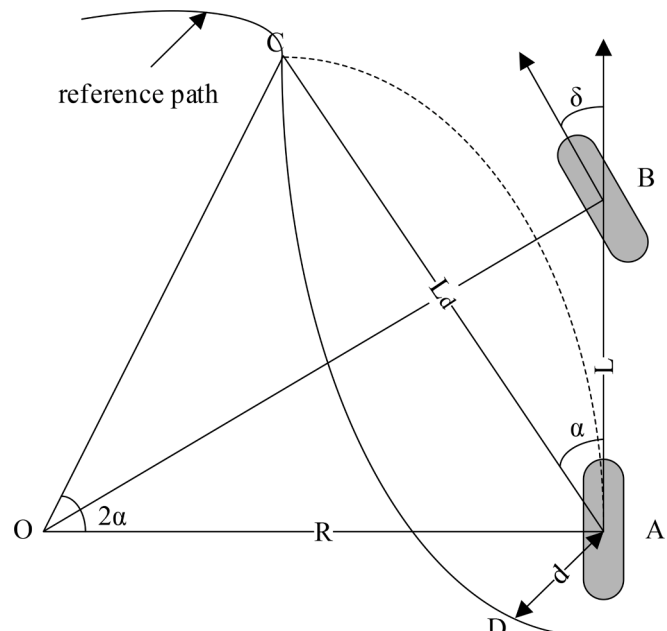
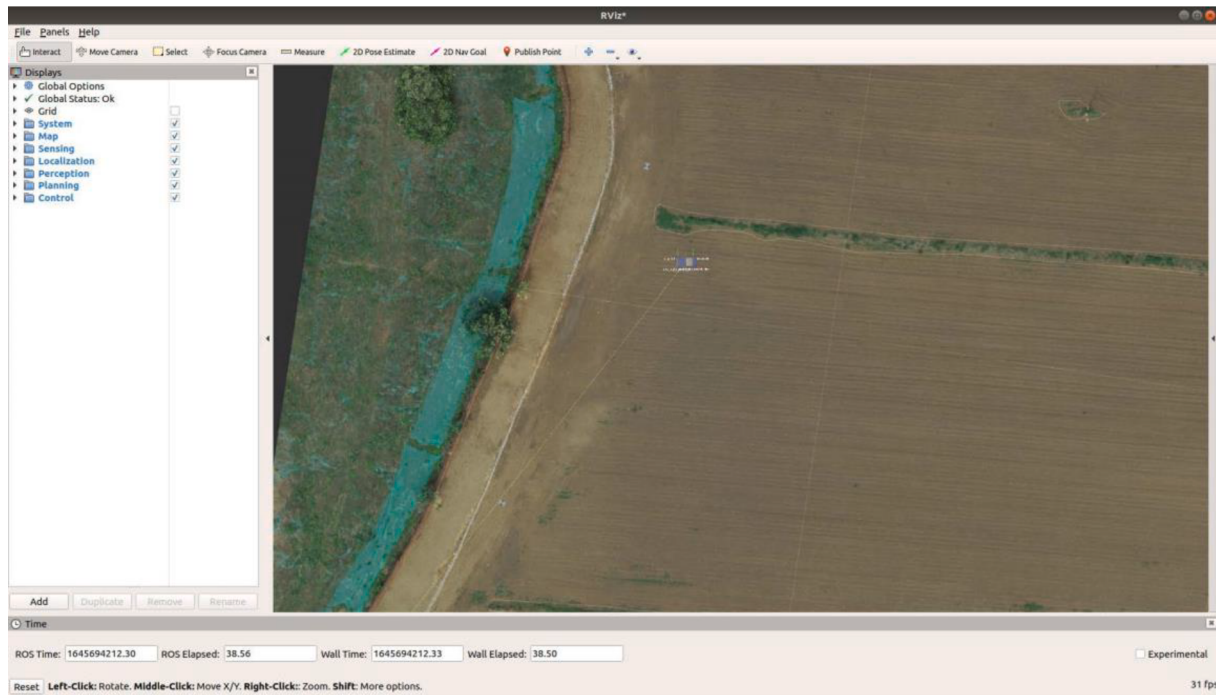
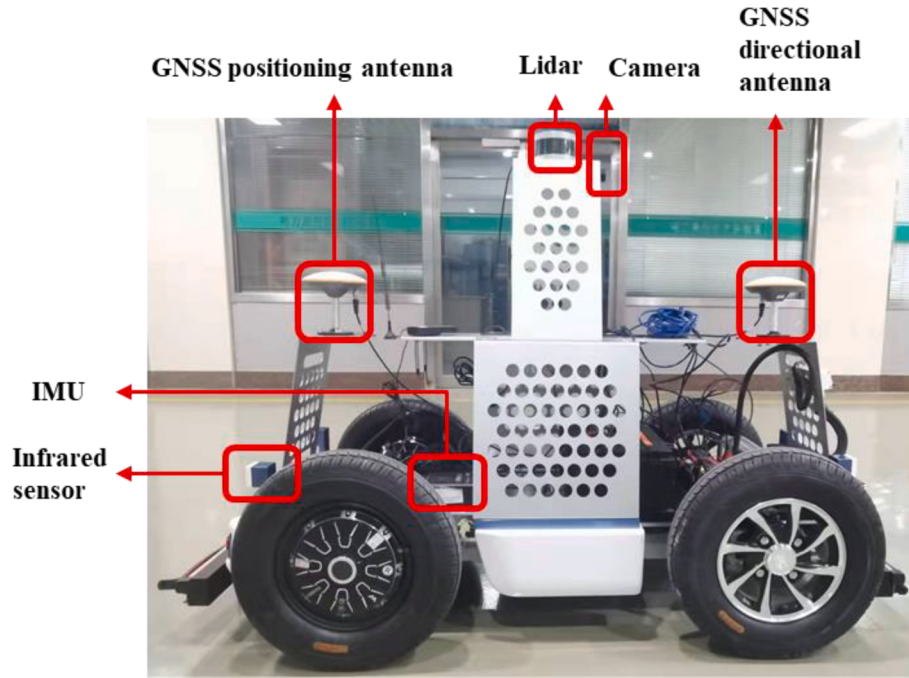


Fig. 9. Pure pursuit algorithm.



**Fig. 10.** Simulation Platform. The simulation platform is constructed to the same scale as the real-world environment, making it suitable for simulating the motion algorithms of agricultural machinery.



**Fig. 11.** Mobile platform with GNSS/IMU, which is used for obstacle avoidance algorithm validation.

Reeds and Shepp. (1990) developed a shortest path planner for car-like vehicles using lines and circles, which we take as the initial path generation method, as shown in Fig. 5. When the center of the OFC is in a field-work track, we select the direction of the unoperated field-work track; otherwise, we prioritize choosing the direction of the inferior arc.

Here,  $XOY$  is the tractor coordinate system,  $AB$  is the field-work track, and  $O$  is the OFC with radius  $r_{min}$  (minimum turn radius of the tractor).  $O_1$  and  $O_2$  are tangent to the two tangents  $PC$  and  $PD$  to  $H$  and  $J$ , and the two circles are tangent to the  $AB$  line to  $G$  and  $I$ .  $PC$  and  $PD$  are

tangent to  $OFC E$  and  $F$ . The curved section  $GHEFJI$  constitutes the initial obstacle avoidance trajectory, which has a low computational cost. Optimization is needed to generate a feasible and jerk-free path where the trajectory is not continuous.

#### 2.1.3. The minimum snap algorithm with path optimization

Because the problem focuses on accurate agricultural path planning, some tractor constraints that may limit the trajectories codified into the courses must be considered. Accordingly, the fundamental obstacle

**Table 1**

Main parameters of the mobile platform.

| Parameters             | Unit | Value        |
|------------------------|------|--------------|
| External dimensions    | mm   | 1608*800*510 |
| Wheelbase              | mm   | 900          |
| Front-wheel Tread      | mm   | 686          |
| Rear-wheel Tread       | mm   | 692          |
| Speed                  | km/h | 0-50         |
| Front Wheel Rotation   | °    | -27°-27°     |
| Minimum turning radius | mm   | 240          |

**Table 2**

CGI-610 IMU main parameters.

| Parameters                 | Unit | Value      |
|----------------------------|------|------------|
| Positioning accuracy (RTK) | cm   | 1          |
| Attitude accuracy          | °    | 900        |
| Output Frequency           | Hz   | 100        |
| Initialization time        | s    | 60         |
| External dimensions        | mm   | 162*120*53 |
| Weight                     | kg   | 0.5        |

avoidance path is difficult to represent as a polynomial function, so it will be a piecewise polynomial as a function of time  $T$ . A higher-order polynomial function can represent each curve segment as (1).

$$p(t) = a_0 + a_1 t + a_2 t^2 + \dots + a_n t^n = \sum_{i=0}^n a_i t^i \quad (1)$$

where  $a_0, a_1, \dots, a_n$  are the trajectory parameters,  $t$  is time, and  $n$  is the polynomial order. Let the parameter vector  $p = [a_0, a_1, \dots, a_n]^T$ ; then, the corresponding trajectory can be expressed as (2).

$$p(t) = \begin{cases} [1, t, t^2, \dots, t^n] \cdot p_1 & T_0 \leq t < T_1 \\ [1, t, t^2, \dots, t^n] \cdot p_2 & T_1 \leq t < T_2 \\ \dots \\ [1, t, t^2, \dots, t^n] \cdot p_k & T_{k-1} \leq t < T_k \end{cases} \quad (2)$$

where  $k$  is equal to the initial obstacle avoidance waypoints minus one.

**Table 3**

Main parameters of the tractor.

| Parameters                   | Unit  | Value          |
|------------------------------|-------|----------------|
| External dimensions          | mm    | 5817*2913*3550 |
| Wheelbase                    | mm    | 3042           |
| Front-wheel Tread            | mm    | 1920           |
| Rear-wheel Tread             | mm    | 1900           |
| Speed                        | km/h  | 0.4-35.22      |
| Rated power of diesel engine | kw    | 162            |
| Rated speed of diesel engine | r/min | 2200           |
| Minimum turning radius       | mm    | 500            |

For any time  $t$ , the position  $P$ , velocity  $v$ , acceleration  $a$ , jerk, snap, etc., of the trajectory can be calculated according to the parameters shown as (3).

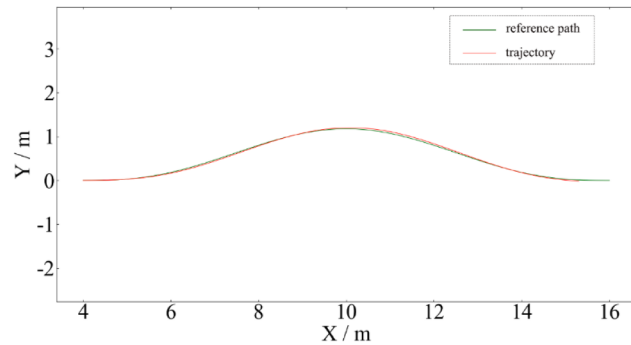
$$\left\{ \begin{array}{l} v(t) = p^{(1)}(t) = [0, 1, 2t, 3t^2, 4t^3, \dots, nt^{n-1}]p \\ a(t) = p^{(2)}(t) = [0, 0, 2, 6t, 12t^2, \dots, n(n-1)t^{n-2}]p \\ \text{jerk}(t) = p^{(3)}(t) = [0, 0, 0, 6, 24t, \dots, \frac{n!}{(n-3)!}t^{n-3}]p \\ \text{snap}(t) = p^{(4)}(t) = [0, 0, 0, 0, 24, \dots, \frac{n!}{(n-4)!}t^{n-4}]p \end{array} \right. \quad (3)$$

In prior literature, the minimum jerk method and minimum snap algorithms are commonly used in numerical optimization (Zha et al., 2021)(De Almeida and Akella, 2017). The minimum jerk algorithm can be used to solve for the minimum acceleration rate, which is conducive to enhancing the comfort of the tractor.

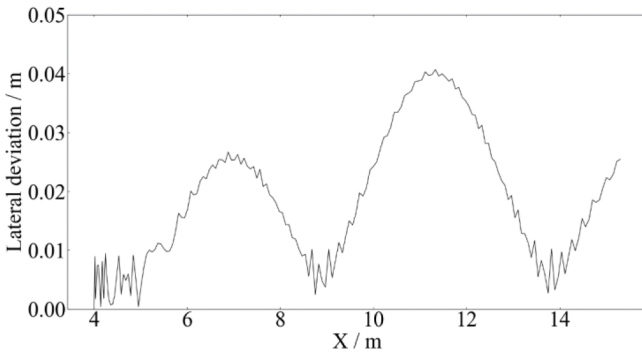
**2.1.3.1. Equality constraints.** When constructing the optimal objective function for the best obstacle avoidance path, we must find constraints to solve for its coefficients. Equality constraints in Equations (4)-(6) constrain orientation, position, velocity, or angular velocity via waypoints and enforce continuity and its derivatives.



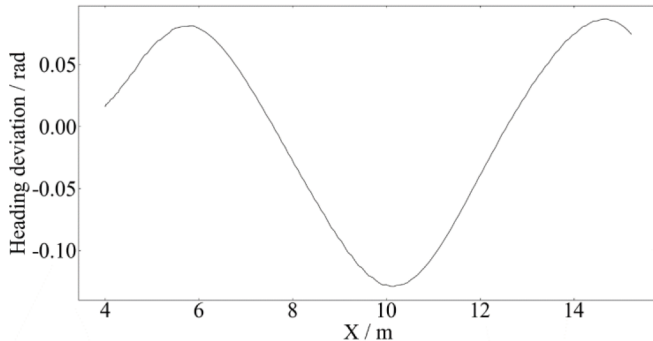
**Fig. 12.** DF2204 tractor. Experimental equipment, an automatic navigation tractor with CVT, GNSS/IMU, steering wheel motor, and angle sensors.



(a) The reference path and tracking trajectory



(b) Variation of lateral deviation



(c) Variation of heading deviation

**Fig. 13.** Schematic diagram of simulation tracking trajectory, variation of lateral deviation, and heading deviation at  $v = 1.5 \text{ m/s}$ .

$$\left\{ \begin{array}{l} [1, t_0, t_0^2, \dots, t_0^n, \underbrace{0 \dots 0}_{(k-1)(n+1)}] p = [x_0, y_0] \\ [0, 1, 2t_0, \dots, nt_0^{n-1}, \underbrace{0 \dots 0}_{(k-1)(n+1)}] p = [v_{0x}, 0] \\ [0, 0, 2, \dots, n(n-1)t_0^{n-2}, \underbrace{0 \dots 0}_{(k-1)(n+1)}] p = [0, 0] \\ [0, 0, 0, 6, \dots, n(n-1)(n-2)t_0^{n-3}, \underbrace{0 \dots 0}_{(k-1)(n+1)}] p = [0, 0] \end{array} \right. \quad (4)$$

where  $[x_0, y_0]$  is the coordinate of the starting point, and the

trajectory should start with the velocity, acceleration, and jerk equal to zero.

$$\left\{ \begin{array}{l} [\underbrace{0 \dots 0}_{(k-1)(n+1)}, 1, t_k, t_k, \dots, t_k^n] p = [x_k, y_k] \\ [\underbrace{0 \dots 0}_{(k-1)(n+1)}, 0, 1, 2t_k, \dots, nt_k^{n-1}] p = [v_{kx}, 0] \\ [\underbrace{0 \dots 0}_{(k-1)(n+1)}, 0, 0, 2, \dots, n(n-1)t_k^{n-2}] p = [0, 0] \\ [\underbrace{0 \dots 0}_{(k-1)(n+1)}, 0, 0, 0, 6, \dots, n(n-1)(n-2)t_k^{n-3}] p = [0, 0] \end{array} \right. \quad (5)$$

where  $[x_k, y_k]$  is the ending point coordinate, and the trajectory should end with the velocity, acceleration, and jerk being equal to zero. The trajectory should be continuous, and therefore, we should impose continuity constraints on the velocity, acceleration, and higher derivatives:

$$\left\{ \begin{array}{l} [\underbrace{0 \dots 0}_{(i-1)(n+1)}, 1, t_i, t_i^2, \dots, t_i^n, -1, -t_i, -t_i^2, \dots, -t_i^n, \underbrace{0 \dots 0}_{(k-i-1)(n+1)}] p = 0 \\ [\underbrace{0 \dots 0}_{(i-1)(n+1)}, 0, 1, 2t_i, \dots, nt_i^{n-1}, 0, -1, -2t_i, \dots, -nt_i^{n-1}, \underbrace{0 \dots 0}_{(k-i-1)(n+1)}] p = 0 \\ [\underbrace{0 \dots 0}_{(i-1)(n+1)}, 0, 0, 2, \dots, \frac{n!}{(n-2)!} t_i^{n-2}, 0, 0, -2, \dots, -\frac{n!}{(n-2)!} t_i^{n-2}, \underbrace{0 \dots 0}_{(k-i-1)(n+1)}] p = 0 \\ [\underbrace{0 \dots 0}_{(i-1)(n+1)}, 0, 0, 0, 6, \dots, \frac{n!}{(n-3)!} t_i^{n-3}, 0, 0, 0, -6, \dots, -\frac{n!}{(n-3)!} t_i^{n-3}, \underbrace{0 \dots 0}_{(k-i-1)(n+1)}] p = 0 \end{array} \right. \quad (6)$$

**2.1.3.2. Inequality constraints.** If only the equation constraint is added, it does not guarantee the safety of obstacle avoidance. Inequality constraints are added to enforce safety constraints such as collision avoidance and curvature. We increase the optimization area to limit the optimal range of the obstacle avoidance path, as shown in Fig. 6. Considering the complexity of the calculation, the optimization area can be chosen as a square, rectangle, or diamond.

The radius of the optimization square is 0.5 m. Additionally, the initial waypoints are far away from each other, overconstraining the problem; they need to be filled with  $n$  path points between every two initial waypoints, as shown in Equation (7).

$$n = \lceil \lceil (x_i - x_{i+1})^2 + (y_i - y_{i+1})^2 \rceil / r \rceil + 1 \quad (7)$$

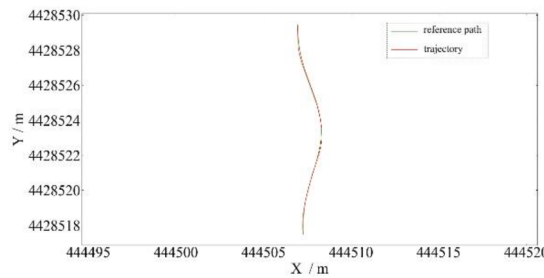
where  $[x_i, y_i]$  and  $[x_k, y_k]$  are the  $i^{\text{th}}$  and  $(i+1)^{\text{th}}$  point coordinates, and  $r$  is the radius of the optimization square. Then, the optimized coordinates  $[p_{ix}(t), p_{iy}(t)]$  should meet inequality (8).

$$\begin{cases} x_{\min} \leq p_{ix}(t) \leq x_{\max} \\ y_{\min} \leq p_{iy}(t) \leq y_{\max} \end{cases} \quad (8)$$

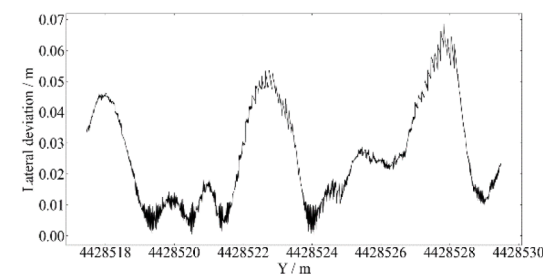
where  $[x_{\min}, y_{\min}]$  and  $[x_{\max}, y_{\max}]$  are the upper and lower bounds of the optimization area, respectively.

Many prior studies considered shortening the length or meeting the position continuity, direction continuity, curvature continuity, etc., of the obstacle avoidance path, without considering the maximum curvature of the obstacle avoidance path. The front wheel steering range of agricultural machinery is limited by the maximum front wheel turning angle. When the curvature of the obstacle avoidance path exceeds the range of the maximum front wheel turning angle, the tracking process will reduce tracking accuracy due to understeering, which will affect the quality and safety of the operation. Therefore, the maximum curvature of the given path  $K_{\max}$  should be less than the reciprocal of the minimum turning radius  $R_{\min}$ , as shown in (9).

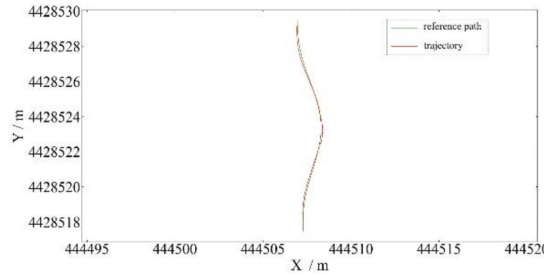
$$K_{\max} \leq \frac{1}{R_{\min}} \quad (9)$$



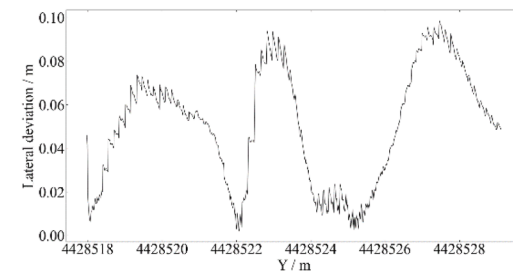
(a) reference path and trajectory (0.5 m/s)



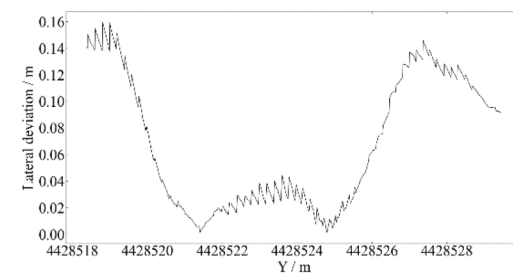
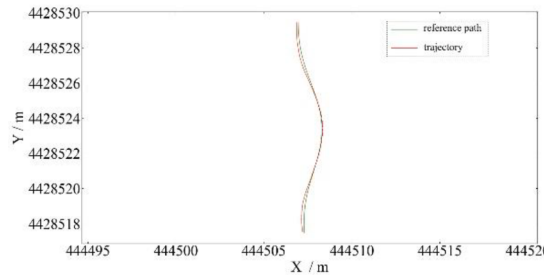
(b) variation of lateral deviation (0.5 m/s)



(c) reference path and trajectory (0.8 m/s)



(d) variation of lateral deviation (0.8 m/s)

**Fig. 14.** Mobile platform tracking trajectory and dynamic change in lateral deviation.

If the obstacle avoidance curve is given by the Equation  $y = f(x)$ ,  $K$  can be given as:

$$K = \frac{|y''|}{(1 + y^2)^{3/2}} \quad (10)$$

Since the tractor must track discrete points, the curvature of the discrete points is given by the curvature circle, as shown in Fig. 7.

Here,  $P_0$ ,  $P_1$ ,  $P_2$  lie on the circle  $O$ , and  $\overrightarrow{P_1P_3}$  is the vector sum of  $\overrightarrow{P_1P_0}$  and  $\overrightarrow{P_1P_2}$ . When  $\alpha \rightarrow 0$ ,  $|\overrightarrow{P_1P_0}|$  and  $|\overrightarrow{P_1P_2}|$  are approximately equal to the arc length, according to the formula:

$$\alpha = \Delta s/R \quad (11)$$

In triangle  $OP_0P_1$  and quadrilateral  $P_0P_1P_2P_3$ , the geometric relationship is given as (12).

$$|\overrightarrow{P_1P_3}| = \Delta s \cdot \alpha \quad (12)$$

Then, it is given by (13).

$$|\overrightarrow{P_1P_3}| = \Delta s^2/R \quad (13)$$

Satisfying the curvature constraint means that  $|\overrightarrow{P_1P_3}| \leq R_{\min}$ . For the

entire given discrete path point, the following Formula (14) is derived:

$$(x_{i-1} + x_{i+1} - 2x_i)^2 + (y_{i-1} + y_{i+1} - 2y_i)^2 \leq (\Delta s^2 \cdot K_{\max})^2 \quad (14)$$

**2.1.3.3. Solution methodology.** This problem can be written in the following quadratic programming form:

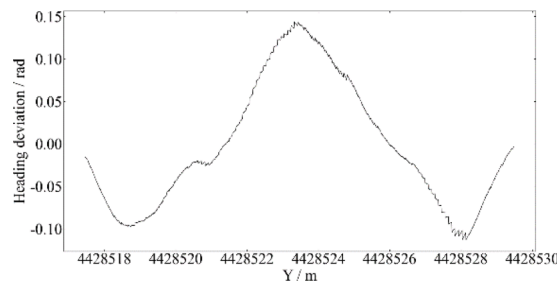
$$\begin{cases} \min_{p, \delta t} J(\delta t) = p^T Q p \\ \text{s.t.} \quad A_{eq} p = b_{eq} \\ \quad \quad A_{ineq} p \leq b_{ineq} \end{cases} \quad (15)$$

The matrices  $A_{eq}$ ,  $A_{ineq}$ , and  $Q$  are functions of time allocation.  $Q$  and  $Q_i$  can be expressed as:

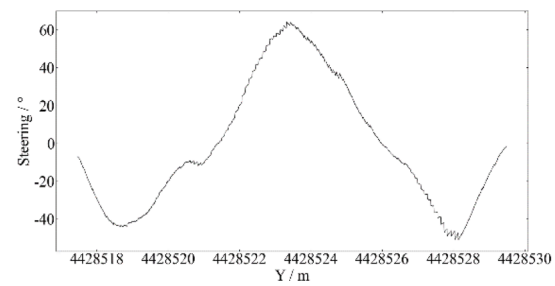
$$Q = \begin{bmatrix} Q_1 & & & \\ & Q_2 & & \\ & & \ddots & \\ & & & Q_k \end{bmatrix} \quad (16)$$

$$Q_i = \begin{bmatrix} 0_{4 \times 4} & r! & c! & 1 \\ 0_{(n-3) \times 4} & (r-4)! & (c-4)! & (r-4) + (c-4) + 1 \end{bmatrix} (t_i^{r+c-7} - t_{i-1}^{r+c-7})^{(n+1) \times (n+1)} \quad (17)$$

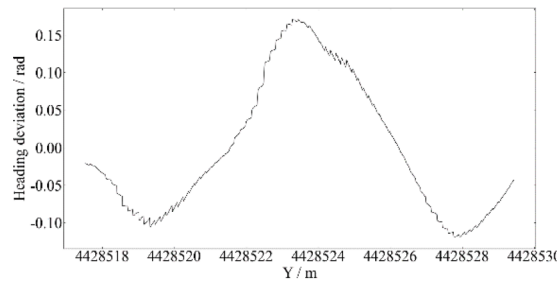
The solving platform is MATLAB R2021a as the QP solver.



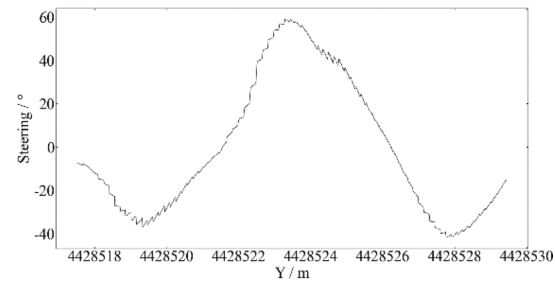
(a) heading deviation (0.5 m/s)



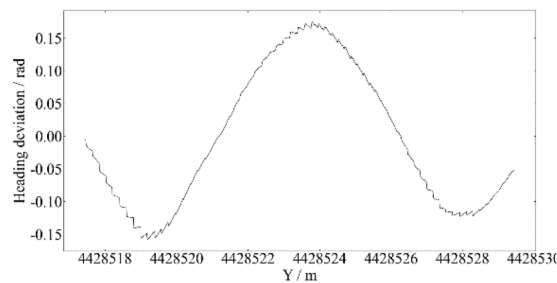
(b) variation of front steering (0.5 m/s)



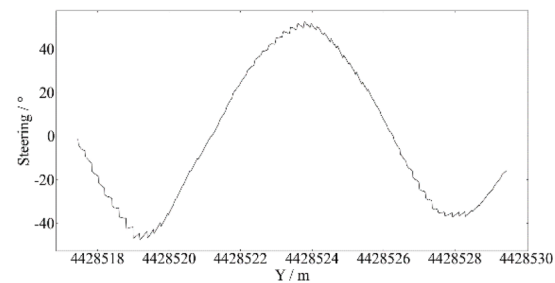
(c) heading deviation (0.8 m/s)



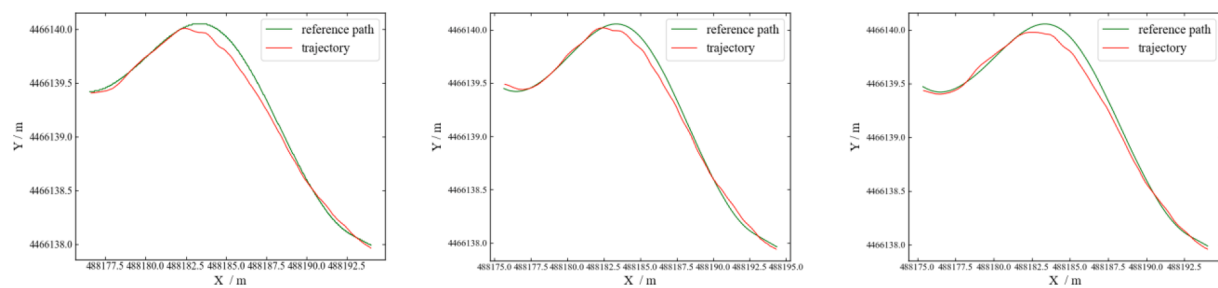
(d) variation of front steering (0.8 m/s)



(e) heading deviation (1.0 m/s)



(f) variation of front steering (1.0 m/s)

**Fig. 15.** Mobile platform heading deviation and variation of front steering.**Fig. 16.** Tractor tracking trajectory at  $v = 0.6 \text{ m/s}$ ,  $v = 0.8 \text{ m/s}$ , and  $v = 1.0 \text{ m/s}$ .

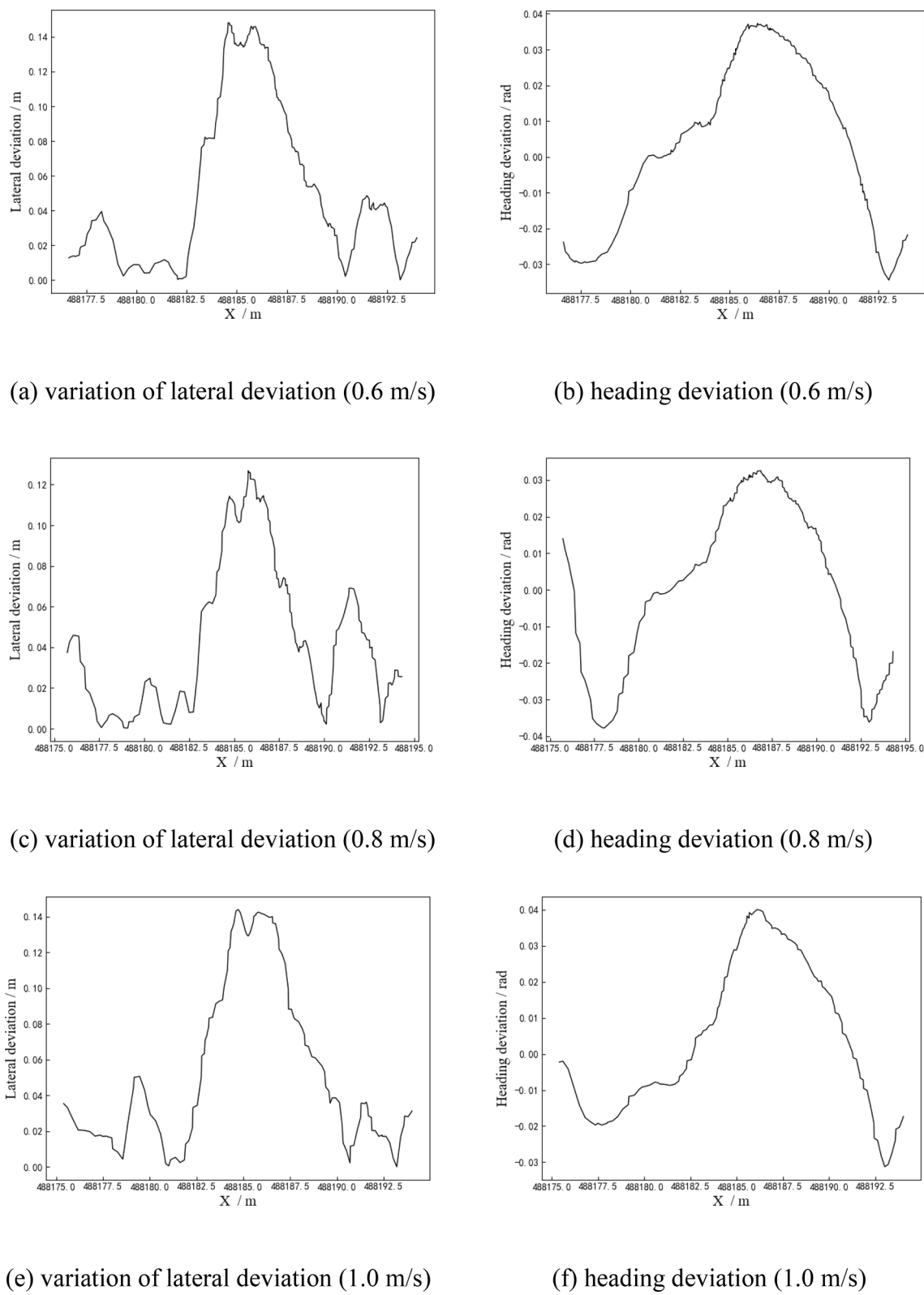


Fig. 17. Tractor dynamic change of lateral deviation and head deviation.

## 2.2. Simulation studies of the algorithm on ROS

In this subsection, the motion model of the tractor is introduced, and ROS simulation is conducted to verify the usability of the obstacle avoidance path planner.

### 2.2.1. Motion model of the tractor

It is assumed that rolling and pitching motions are ignored. The agricultural machinery is simplified to a two-wheel bicycle model. We use the pure pursuit algorithm in the path-tracking control of the autonomous tractor.

**2.2.1.1. Kinematic model.** The bicycle model is often used to express the kinematics of the tractor without considering factors such as aerodynamics or tire sideways deflection, as shown in Fig. 8. It is a 2DOF model where the front and rear wheels are lumped together, and only the front wheel is used for steering. In this model, denote the positions of the front and rear wheels, respectively.  $\varphi$  is the orientation of the tractor in the global reference frame,  $\delta$  is the steering of the front wheel, and  $L$  shows the distance between the front and rear axle points.

The longitudinal velocity of the tractor at the rear wheel  $v_r$  can be expressed as:

$$v_r = \dot{X}_r \cos\varphi + \dot{Y}_r \sin\varphi \quad (18)$$

The nonholonomic constraint for each wheel can be expressed as:

$$\begin{cases} \dot{X}_f \sin(\varphi + \delta) - \dot{Y}_f \cos(\varphi + \delta) = 0 \\ X_f \sin\varphi - Y_f \cos\varphi = 0 \end{cases} \quad (19)$$

With the rigid body constraint between the front and rear wheels, we have:

$$\begin{cases} X_f = X_r + L \cos\varphi \\ Y_f = Y_r + L \sin\varphi \end{cases} \quad (20)$$

Combining (18), (19), and (20), the kinematic model of the tractor can be obtained:

$$\begin{bmatrix} \dot{X}_r \\ \dot{Y}_r \\ \dot{\varphi} \end{bmatrix} = \begin{bmatrix} \cos\varphi & \sin\varphi & 0 \\ \sin\varphi & \cos\varphi & 0 \\ 0 & 0 & \tan\delta/L \end{bmatrix} v_r \quad (21)$$

**2.2.1.2. Pure pursuit algorithm.** The pure pursuit algorithm is a typical control algorithm for path-tracking agricultural machines (Yang et al., 2022b), and the achievement is shown in Fig. 9. It regards the rear axle center  $A$  as the tangent point and the body as the tangent line, and controls the front wheel angle so that  $A$  follows the given curve that smoothly passes through the goal point  $C$ .  $L_d, B, D, L, \alpha$ , and  $d$  are the look-ahead distance, front axle center, trajectory point closest to  $A$ , wheelbase, steering deviation, and lateral deviation, respectively.

For the rear axle center  $A$  to reach the destination  $C$ , in  $\triangle OAC$ , we have:

$$\frac{L_d}{\sin 2\alpha} = \frac{R}{\sin(\pi/2 - \alpha)} \quad (22)$$

From the geometric relationship, it is clear that:

$$\delta = \arctan(2L \sin\alpha / L_d) \quad (23)$$

### 2.2.2. The virtual robotic platform

The simulation environment uses ROS Melodic as the system architecture. The 3D model of the field as generated from aerial footage is loaded into Autoware, which is built on ROS and enables commercial deployment of autonomous driving in a broad range of vehicles and applications. We created an isometric 3D model of the tractor in the Unified Robot Description Format (URDF) in the Gazebo 3D scenery environment. The interface for visualization using Rviz is shown in

Fig. 10.

### 2.3. Mobile platform validation

A mobile platform validation was conducted to investigate the effects of using the obstacle avoidance trajectory, as shown in Fig. 11. The main parameters of the tractor test platform are shown in Table 1.

The GNSS/IMU has a built-in MEMS gyroscope and accelerometer and supports external odometer information for assistance, which can provide real-time high-precision information on the position and speed of the mobile platform. The main parameters are shown in Table 2.

The mission plan is defined in a CSV formatted file. The CSV file is uploaded to the autonomous vehicle through the user interface. The mobile platform uses a Controller Area Network (CAN) to communicate with the onboard computer. Comparison experiments with driving speeds of 0.5 m/s, 0.8 m/s and 1.0 m/s were conducted. Three tests were performed at different speeds, and results were obtained.

### 2.4. Field experiment

The DF2204 autonomous tractor, developed in cooperation with the China Agriculture University (CAU), was used as the experimental platform for the obstacle avoidance test. We set up path-tracking experiments in the field, as shown in Fig. 12. Consistent with the simulator, the pure pursuit algorithm was applied to the navigation controller to calculate the steering angle. The main parameters of the tractor are shown in Table 3.

To validate whether the autonomous tractor could follow the obstacle avoidance path at an acceptable level, the operating velocities were set to 0.6 m/s, 0.8 m/s, and 1.0 m/s. The lateral deviation was obtained from the IMU by comparing the tracking waypoints with the reference path, and the values of the heading deviations were measured.

## 3. Results and discussion

### 3.1. Simulation results

The obstacle avoidance operation examples were presented to demonstrate the path planning method.

In Fig. 13 (a), the green path is the reference path, and the red path is the tracking trajectory. The simulation result shows that the tracking path of the tractor is essentially the same as the predefined path. As shown in Fig. 13(b), the maximum value of the lateral deviation is 4.07 cm, the mean value is 1.75 cm, and the average root means the square error is 1.12 cm, which meets the accuracy requirements of obstacle avoidance tracking. As shown in Fig. 13(c), the steering error is in the range of  $-0.12 \sim 0.10$  rad. The simulation results show that the developed obstacle avoidance path planning method can realize the autonomous obstacle avoidance of farm machinery.

### 3.2. Mobile platform results

According to Fig. 14(a), (c), and (e), the points with large lateral deviation are mainly concentrated in the path direction changing. The statistical analysis of the lateral deviation is shown in Fig. 14 (b), (d), and (f), with a mean value of 4.81 cm and an overall standard deviation of 3.07 cm.

Fig. 15 shows that the points with larger heading deviation are concentrated at the positions with larger path curvature. The heading deviation is located at  $-0.159 \sim 0.174$  rad. The front steering and heading deviations trend in the same direction, and the maximum values range from  $-120^\circ$  to  $120^\circ$ , which meets the tracking requirements.

### 3.3. Analysis of field test results

The tractor velocity was set to 0.6 m/s, 0.8 m/s, and 1.0 m/s. The

tracking process is shown in Fig. 15. According to Fig. 16, the average values of the lateral error for obstacle avoidance are 0.052 m, 0.051 m, and 0.061 m, and the average root mean square errors are 0.061 m, 0.039 m, and 0.048 m, corresponding to speeds of 0.6 m/s, 0.8 m/s, and 1.0 m/s, respectively. At these three speeds, the heading deviations of the tractor are in the range of  $-0.034$  rad to  $0.037$  rad,  $-0.038$  rad to  $0.033$  rad, and  $-0.031$  rad to  $0.040$  rad as shown in Fig. 17. Compared with other related studies, this study conducted field experiments on agricultural machines and showed better performance in terms of heading deviation and lateral deviation (Liu et al., 2018). The above field tests show that the algorithm proposed in this paper can track obstacle avoidance paths safely and smoothly with the pure pursuit algorithm.

#### 4. Conclusion

In this study, an obstacle avoidance path planner was developed to generate a path for a tractor in the field by applying the minimum snap algorithm. The constraints of different stages of autonomous obstacle avoidance are analyzed, and the initial obstacle avoidance path to be optimized is obtained using the improved shortest tangent method after simplifying the obstacles. Convex quadratic programming is used to optimize the obstacle avoidance path that meets safety requirements, continuous smoothness, and kinematic constraints for path tracking. We have built a robot simulation platform for agricultural machine simulation and real experiments. The real experiment was conducted on the mobile platform and tractor, verifying the feasibility of the proposed algorithm. Results showed that the average root means the square error of the obstacle avoidance path tracking was 0.049 m, the average lateral deviation was 0.055 m, and the effect was favorable. In the future, we will focus on optimizing dynamic obstacle avoidance algorithms for complex environments, such as roads between farmlands.

#### CRediT authorship contribution statement

**Xin Zhao:** Methodology, Writing – original draft, Writing – review & editing. **Ke Wang:** Software, Validation. **Sixian Wu:** Data curation, Visualization. **Long Wen:** Conceptualization. **Zhibo Chen:** Conceptualization, Writing – review & editing. **Liang Dong:** Analysis and interpretation of data. **Mengyao Sun:** Project administration. **Caicong Wu:** Supervision, Project administration.

#### Declaration of Competing Interest

The authors declare that they have no known competing financial interests or personal relationships that could have appeared to influence the work reported in this paper.

#### Data availability

Data will be made available on request.

#### Acknowledgments

This work has been funded by Beijing Municipal Science and Technology Project (Grant number: Z201100008020008) and the National Key Research & Development Project (Grant number: 2021YFB3901302); The authors thank The Graduate Student Miyun Henanzhai Practice Base of China Agriculture University.

#### References

- Abdallaoui, S., Aglizim, E.H., Chaibet, A., Kribèche, A., 2022. Thorough Review Analysis of Safe Control of Autonomous Vehicles: Path Planning and Navigation Techniques. *Energies* 15. <https://doi.org/10.3390/en15041358>.
- Bochtis, D., Griepentrog, H.W., Vougioukas, S., Busato, P., Berruto, R., Zhou, K., 2015. Route planning for orchard operations. *Comput. Electron. Agric.* 113, 51–60. <https://doi.org/10.1016/j.compag.2014.12.024>.
- Bochtis, D.D., Sørensen, C.G., 2009. The vehicle routing problem in field logistics part I. *Biosyst. Eng.* 104, 447–457. <https://doi.org/10.1016/j.biosystemseng.2009.09.003>.
- Bochtis, D.D., Vougioukas, S.G., 2008. Minimising the non-working distance travelled by machines operating in a headland field pattern. *Biosyst. Eng.* 101, 1–12. <https://doi.org/10.1016/j.biosystemseng.2008.06.008>.
- Bohren, J., Foote, T., Keller, J., Kushleyev, A., Lee, D., Stewart, A., Vernaza, P., Derenick, J., Spletzer, J., Satterfield, B., 2008. Little Ben: The Ben Franklin Racing Team's entry in the 2007 DARPA Urban Challenge. *J. F. Robot.* 25, 598–614. <https://doi.org/10.1002/rob.20260>.
- Chabini, I., Lan, S., 2002. Adaptations of the A\* Algorithm for the Computation of Fastest Paths in Deterministic Discrete-Time Dynamic Networks. *IEEE Trans. Intell. Transp. Syst.* 3, 60–74. <https://doi.org/10.1109/6979.994796>.
- De Almeida, M.M., Akella, M., 2017. New numerically stable solutions for minimum-snap quadcopter aggressive maneuvers. *Proc. Am. Control Conf.* 1322–1327. 10.23919/ACC.2017.7963135.
- Godoy, J., Artuñedo, A., Beteta, M., Villagra, J., 2022. Corridors-based navigation for automated vehicles convoy in off-road environments\*. *IFAC-PapersOnLine* 55, 71–76. <https://doi.org/10.1016/ifacol.2022.07.585>.
- González, D., Pérez, J., Milanés, V., Nashashibi, F., 2016. A Review of Motion Planning Techniques for Automated Vehicles. *IEEE Trans. Intell. Transp. Syst.* 17, 1135–1145. <https://doi.org/10.1109/TITS.2015.2498841>.
- Hameed, I.A., 2018. Coverage path planning software for autonomous robotic lawn mower using Dubins' curve. *2017 IEEE Int. Conf. Real-Time Comput. Robot. RCAR* 2017–July, 517–522. 10.1109/RCAR.2017.8311915.
- He, P., Li, J., Zhang, D., Wan, S., 2018. Optimisation of the harvesting time of rice in moist and non-moist dispersed fields. *Biosyst. Eng.* 170, 12–23. <https://doi.org/10.1016/j.biosystemseng.2018.03.008>.
- Jeon, C.W., Kim, H.J., Yun, C., Gang, M.S., Han, X., 2021. An entry-exit path planner for an autonomous tractor in a paddy field. *Comput. Electron. Agric.* 191, 106548. <https://doi.org/10.1016/j.compag.2021.106548>.
- Kavraki, L.E., Švestka, P., Latombe, J.C., Overmars, M.H., 1996. Probabilistic roadmaps for path planning in high-dimensional configuration spaces. *IEEE Trans. Robot. Autom.* 12, 566–580. <https://doi.org/10.1109/70.508439>.
- LaValle, S.M., Kuffner, J.J., 2001. Randomized Kinodynamic Planning. *Int. J. Rob. Res.* 20, 378–400. <https://doi.org/10.1177/02783640122067453>.
- Lei, T., Luo, C., Jan, G.E., Bi, Z., 2022. Deep Learning-Based Complete Coverage Path Planning With Re-Joint and Obstacle Fusion Paradigm. *Front. Robot. AI* 9. <https://doi.org/10.3389/frobt.2022.843816>.
- Liu, C., Zhao, X., Du, Y., Cao, C., Zhu, Z., Mao, E., 2018. Research on static path planning method of small obstacles for automatic navigation of agricultural machinery. *IFAC-PapersOnLine* 51, 673–677. <https://doi.org/10.1016/j.ifacol.2018.08.119>.
- Ma, Z., Yin, C., Du, X., Zhao, L., Lin, L., Zhang, G., Wu, C., 2022. Rice row tracking control of crawler tractor based on the satellite and visual integrated navigation. *Comput. Electron. Agric.* 197, 106935 <https://doi.org/10.1016/j.compag.2022.106935>.
- Moysiadis, V., Tsolakis, N., Katikaridis, D., Sørensen, C.G., Pearson, S., Bochtis, D., 2020. Mobile robotics in agricultural operations: A narrative review on planning aspects. *Appl. Sci.* 10 <https://doi.org/10.3390/app10103453>.
- Oksanen, T., Visala, A., 2009. Coverage path planning algorithms for agricultural field machines. *J. F. Robot.* 26, 651–668.
- Reeds, J., Shepp, L., 1990. Optimal paths for a car that goes both forwards and backwards. *Pacific J. Math.* 145, 367–393.
- Santos, L., Santos, F.N., Magalhaes, S., Costa, P., Reis, R., 2019b. Path Planning approach with the extraction of Topological Maps from Occupancy Grid Maps in steep slope vineyards. *19th IEEE Int. Conf. Auton. Robot Syst. Compet. ICARSC* 2019. 10.1109/ICARSC.2019.8733630.
- Santos, L., Santos, F., Mendes, J., Costa, P., Lima, J., Reis, R., Shinde, P., 2019. Path Planning Aware of Robot's Center of Mass for Steep Slope Vineyards. *Robotica* 38, 684–698. <https://doi.org/10.1017/S0263574719000961>.
- Santos, L.C., Santos, F.N., Valente, A., Sobreira, H., Sarmento, J., Petry, M., 2022. Collision Avoidance Considering Iterative Bézier Based Approach for Steep Slope Terrains. *IEEE Access* 10, 25005–25015. <https://doi.org/10.1109/ACCESS.2022.3153496>.
- Thamrin, N.M., Arshad, N.H.M., Adnan, R., Sam, R., 2022. Forward Navigation for Autonomous Unmanned Vehicle in Inter-Row Planted Agriculture Field BT - Control Engineering in Robotics and Industrial Automation: Malaysian Society for Automatic Control Engineers (MACE) Technical Series 2018, in: Mariappan, M., Arshad, M.R., Akmelialiati, R., Chong, C.S. (Eds.), Springer International Publishing, Cham, pp. 183–198. 10.1007/978-3-030-74540-0-7.
- Utamima, A., Reiners, T., Ansariopoor, A., Seyyedhasani, H., 2018. The agricultural routing planning in field logistics, in: Contemporary Approaches and Strategies for Applied Logistics. IGI Global, pp. 261–283.
- Vougioukas, S., Blackmore, S., Nielsen, J., Fountas, S., 2006. A two-stage optimal motion planner for autonomous agricultural vehicles. *Precis. Agric.* 7, 361–377. <https://doi.org/10.1007/s11119-006-9022-9>.
- Wang, Y., Liu, D., Zhao, H., Li, Y., Song, W., Liu, M., Tian, L., Yan, X., 2022. Rapid citrus harvesting motion planning with pre-harvesting point and quad-tree. *Comput. Electron. Agric.* 202, 107348 <https://doi.org/10.1016/j.compag.2022.107348>.
- Xiong, Y., Ge, Y., Liang, Y., Blackmore, S., 2017. Development of a prototype robot and fast path-planning algorithm for static laser weeding. *Comput. Electron. Agric.* 142, 494–503. <https://doi.org/10.1016/j.compag.2017.11.023>.
- Yang, Y., Li, Y., Wen, X., Zhang, G., Ma, Q., Cheng, S., Qi, J., Xu, L., Chen, L., 2022b. An optimal goal point determination algorithm for automatic navigation of agricultural

- machinery: Improving the tracking accuracy of the Pure Pursuit algorithm. *Comput. Electron. Agric.* 194, 106760. <https://doi.org/10.1016/j.compag.2022.106760>.
- Yang, J., Ni, J., Li, Y., Wen, J., Chen, D., 2022a. The Intelligent Path Planning System of Agricultural Robot via Reinforcement Learning. *Sensors* 22, 1–19. <https://doi.org/10.3390/s22124316>.
- Zha, T., Li, Y., Sun, L., 2021. A Local Planning Method Based on Minimum Snap Trajectory Generation and Traversable Region for Inspection of Airport Roads. 2021 5th Int. Conf. Autom. Control Robot. ICACR 2021, 38–42. <https://doi.org/10.1109/ICACR53472.2021.9605163>.
- Zhang, Z., Zheng, L., Li, Y., Zeng, P., Liang, Y., 2021. Structured road-oriented motion planning and tracking framework for active collision avoidance of autonomous vehicles. *Sci. China Technol. Sci.* 64, 2427–2440. <https://doi.org/10.1007/s11431-021-1880-1>.
- Zhou, K., Leck Jensen, A., Sørensen, C.G., Busato, P., Bothtis, D.D., 2014. Agricultural operations planning in fields with multiple obstacle areas. *Comput. Electron. Agric.* 109, 12–22. <https://doi.org/10.1016/j.compag.2014.08.013>.
- Ziegler, J., Bender, P., Dang, T., Stiller, C., 2014. Trajectory planning for Bertha - A local, continuous method. *IEEE Intell. Veh. Symp. Proc.* 450–457 <https://doi.org/10.1109/IVS.2014.6856581>.